

Finite Element Modeling and Experimental Verification of Nitriding Process in S30C Steel

Xiaohu Deng^{a*}, Dong-ying Ju^b, Min Li^a

^a Tianjin Key Laboratory of high speed cutting and precision machining, Tianjin University of Technology and Education, Tianjin, China

^b Department of Mechanical Engineering, Saitama Institute of Technology, Saitama, Japan

Received: July 13, 2016; Revised: January 05, 2017; Accepted: January 25, 2017

A mathematical model has been developed to simulate the nitriding process of plain carbon steel, considering the simultaneous diffusion of nitrogen in different iron-nitrogen (Fe-N) phases and the precipitation dynamics of γ' and ϵ iron-nitride. The model can predict the distribution of nitrogen concentration, volume fraction of Fe-N phases and hardness. Furthermore, a finite element method (FEM) post-process technology is presented to avoid the limit of FEM mesh improvement and time-saving. The uniform-sum-division algorithm is adopted as local refinement algorithm (LRA) of meshes. The modified inverse distance weighting (IDW) method is used to interpolate the FEM simulated results. Then, the nitriding model and post-process technology are incorporated within the framework of the developed FEM code COSMAP (Computer Simulation of MANufacturing Process) based on metallothermo-mechanical theory. In order to validate the nitriding model and FEM post-process technology, the nitriding process of S30C steel is modeled by COSMAP software. The simulated distributions of nitrogen content and hardness are consistent with the measured ones. In addition, the simulated results at different mesh size are compared for two-dimensional model. It is indicated that the interpolated results agree well with the simulated results of fine mesh model and the experimental ones.

Keywords: *finite element, nitriding, S30C, iron nitride, inverse distance weighting*

1. Introduction

Nitriding is a universal thermochemical heat treatment technology. It involves the diffusion of atomic nitrogen on the surface of a workpiece. The diffusion of nitrogen into steel leads to the formation of thin outer compound layer (white layer) and thick inner diffusion layer. Nitriding technology can be used to improve the hardness, wear resistance and fatigue strength of the surface of steel. Therefore, it is beneficial to know the nitrogen diffusion and transformation kinetics mechanisms in the nitriding process¹.

In the past decades, several models have been developed to predict the nitriding process in steels. In the early 1990s, Somers and Mittemeijer² presented a monolayer and bilayer growth model for the nitriding of pure iron. The model was applied to analyze the growth kinetics of a γ' monolayer on an α -Fe substrate and the growth kinetics of a γ'/ϵ bilayer on an α -Fe substrate. Then, Dimitrov³ developed a diffusion model to predict the compound layer composition and calculated the effective diffusion coefficient. Yan⁴ systematically researched the surface phase constitution and the kinetics of layer growth in pure iron. The growth of a compound layer and diffusion layer, and the nitrogen concentration distribution in the nitrided layers could be precisely predicted by this model. Moreover, Keddams⁵ developed a kinetic model of

nitriding in pure iron by coupling the kinetics data and a thermodynamic description of the Fe-N phase diagram. The model is solved by analytical methods to simulate the diffusion of nitrogen atom and growth of the nitride layer.

However, it is hard to model the nitriding process for irregular geometry and complicated conditions by finite difference or an analytical solution. Cavaliere⁶ modeled the nitriding process by coupling the kinetics data of nitrogen in α , γ' and ϵ phases to the thermodynamic description of the iron-nitrogen (Fe-N) phase diagram respectively. Recently, Hassani-Gangaraj⁷ proposed a finite element simulation to predict the kinetics of layer growth and nitrogen distribution during nitriding according the analogy between diffusion and heat conduction. Both the above models were processed by implementing modifications in the kinetics and modified layers properties into commercial FEM codes. In the present paper, a modified nitriding model is developed by coupling a phenomenological phase transformation dynamic model with the previous developed FEM code COSMAP (Computer Simulation of MANufacturing Process) based on metallothermo-mechanical theory. COSMAP (Computer Simulation of MANufacturing Process) is simulation software for heat treatment process, also capable of carburizing, nitriding and local heating/cooling processes. COSMAP simulates temperature distribution, progressing the phase transformation, stress/strain (distortion) profiles in the manner of the coupling

* e-mail: dengxh@tute.edu.cn

between each other, and chemical composition of carbon and nitrogen in the case of carburizing, and nitriding.

The main purpose is to predict the nitrogen diffusion and mechanical properties during nitriding process of plain carbon steel. Furthermore, a mesh interpolation technology for FEM post-process is developed to simulate the thinner compound layer, saved time and avoided the limit of FEM meshing. The model is applied to simulate the nitriding process in S30C steel, and simulated results are compared with the measured ones.

2. Model Descriptions

In the nitriding of plain carbon steel, the formation of the diffusion layer and its phase compositions are analogous to the characteristics of nitride layer obtained on pure iron. For simplifying the model, it isn't considered that replacement of some nitrogen atoms in the iron-nitrogen phase by larger carbon atoms. The reason is that replacement of some nitrogen atoms by larger carbon atoms causes an increase in the lattice constants, which decreases the diffusion mobility of nitrogen in both ϵ and α phases.

In the present model, the evolution of temperature, nitrogen concentration, microstructure, stress/distortion and hardness can be predicted for the nitriding process of low carbon steel. The detail of introducing heat conduction and diffusion equations is already presented in the previous articles⁸⁻¹⁰. Here, improved equations are summarized in the following.

2.1. The effective diffusion coefficient

An effective diffusion coefficient is employed to avoid the diffusion calculation at the phase boundary. It is dependent on the Fe-N phase structure and corresponding diffusion coefficient, which could be given by the mixture law⁸⁻¹⁰.

$$D_N = \sum D_N^i \xi_i \quad (1)$$

where, for each single phase, $i = 1$ (ϵ), 2 (γ'), 3 (α), D_N^i is diffusivity in various Fe-N phases, ξ_i is the volume fraction of various Fe-N phase. The diffusivity of nitrogen in different Fe-N phase could be approximately expressed in an Arrhenius form^{2,5,7}.

$$\begin{aligned} D_{N,c}^{\alpha} &= (0.586672 + 6.17784 * \exp(-C_c/0.18686)) * \\ &(4.67e-09 * \exp(-75150/(R * T))) \\ D_N^{\gamma'} &= (1.675e-09) * \exp(-64000/(R * T)) \\ D_{N,c}^{\epsilon} &= (1.32612 + 4.57433 * \exp(-C_c/0.18179)) * \\ &(2.27e-05 * \exp(-147600/(R * T))) \end{aligned} \quad (2)$$

where, C_c is the carbon content in the steel, R is the gas constant, and T is the nitriding temperature.

2.2. Phase transformation prediction model

A phenomenological model is developed to calculate the volume fraction of Fe-N phase. The nitriding parameters are connected with the mechanisms of the nitriding process. The volume fraction of Fe-N phases is defined as

$$\begin{aligned} \xi_{\gamma'} \frac{C_N^{i,t} - C_N^{\alpha/\gamma'}}{C_N^{\gamma'/\alpha} - C_N^{\alpha/\gamma'}}, \xi_{\epsilon} &= \xi_{\gamma'} \cdot \frac{C_N^{i,t} - C_N^{\gamma'/\epsilon}}{C_N^{\epsilon/\gamma'} - C_N^{\gamma'/\epsilon}}, \\ \xi_{\alpha} &= 1 - \xi_{\gamma'} - \xi_{\epsilon} \end{aligned} \quad (3)$$

where, $C_N^{i,t}$ is nitrogen concentration, $C_N^{\alpha/\gamma'}$, $C_N^{\gamma'/\alpha}$, $C_N^{\gamma'/\epsilon}$, $C_N^{\epsilon/\gamma'}$ are the limiting nitrogen solubilities in the Fe-N phase as a function of temperature and can be calculated by^{2,5}:

$$\begin{aligned} C_N^{\alpha/\gamma'} &= \exp\left(-\frac{4575}{T} + 3\right) \\ C_N^{\gamma'/\alpha} &= \frac{25.08}{4.25 + 10^{-(\frac{2341.67}{T} - 1.925)}} \\ C_N^{\gamma'/\epsilon} &= \frac{25.08}{4.25 + 10^{-(\frac{3476.67}{T} - 2.455)}} \\ C_N^{\epsilon/\gamma'} &= 3.01 + (1.79 \cdot 10^{-2} T) - (1.54 \cdot 10^{-5} T^2) \end{aligned} \quad (4)$$

2.3. Hardness regression equation

The hardness is mainly dependent on phase structure of steel, which can be calculated by the experimental regression equation

$$HV = HV_{st} + \sum_{x=1}^{n1} a_x C_x + \sum_{y=1}^{n2} b_y \xi_{cy} + \sum_{z=1}^{n3} c_z \xi_{nz} \quad (5)$$

where, HV is the Vickers Hardness, HV_{st} is the Vickers Hardness of the substrate, C_x is the chemical composition, ξ_{cy} is the iron-carbon phase composition, ξ_{nz} is the Fe-N phase composition, and a_x , b_y , c_z are the corresponding weighting coefficients.

2.4. Interpolation model of FEM results

The subdivision is executed on an arbitrary FEM mesh. The FEM mesh can be uniformly divided with high quality and high efficiency by a local refinement algorithm (LRA). The newly generated mesh meets the needs of post-process. FEM simulated results are interpolated by using the modified inverse distance weighting (IDW) interpolation method. The interpolation equation is as following¹¹⁻¹³.

$$N_p = \sum_{i=1}^n l_i^{-u} N_i / \sum_{i=1}^n l_i^{-u} \quad (6)$$

where, N_p is nitrogen concentration of any interpolation points, l_i is the distance between the interpolation points and the nodes, n is the number of nodes.

In the present model, in order to obtain the profiles consistent with FEM results, two modifications have been made for the IDW interpolation function. Firstly, the interpolation is executed successive at points, surfaces and volumes; Secondly, the weighting exponent is set differently for data points to reflect the difference of diffusion coefficients between Fe-N phases.

3. Material and experiments

The material used in this study was a plain carbon steel S30C prepared in the form of cylinder specimens with the diameter of 10mm. Its chemical composition is given in Table 1. Gas nitriding was carried in an industrial unit for an ammonia/hydrogen gas mixture, and the samples were rapid-cooled from the treatment temperature. The heating programme for the nitriding process is shown in Figure 1. A cross-section of the samples was prepared by a standard grinding and polishing procedure and microstructure observations were performed using SEM. Case depth and thickness measurement of the diffusion zone were carried out by optical and scanning electron microscopes and verified with a micro-hardness profile. Hardness measurements on the cross-sections and the surfaces of nitrided specimens were carried out with a Vickers hardness tester. For the determination of nitrogen contents, Electron Probe X-ray Microanalysis (EPMA) was performed on cross-sections of the specimens.

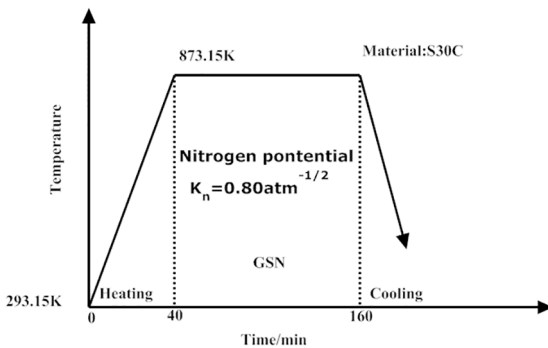


Figure 1. Heating programme of nitriding process.

4. Finite element simulation results and discussions

An axisymmetric finite element model was constructed to simulate the above mentioned nitriding process. Since the specimens' geometry and boundary condition in nitriding were axisymmetric, it can be a reasonable assumption that diffusion takes place in one direction (radial). The boundary condition of heat transfer and nitrogen diffusion

is set up on the red line. A schematic of the specimen and a representative strip as well as the finite element mesh are shown in Figure 2. The series of equations governing the nitriding process, developed above, were numerically solved by the finite element (FEM) code COSMAP.

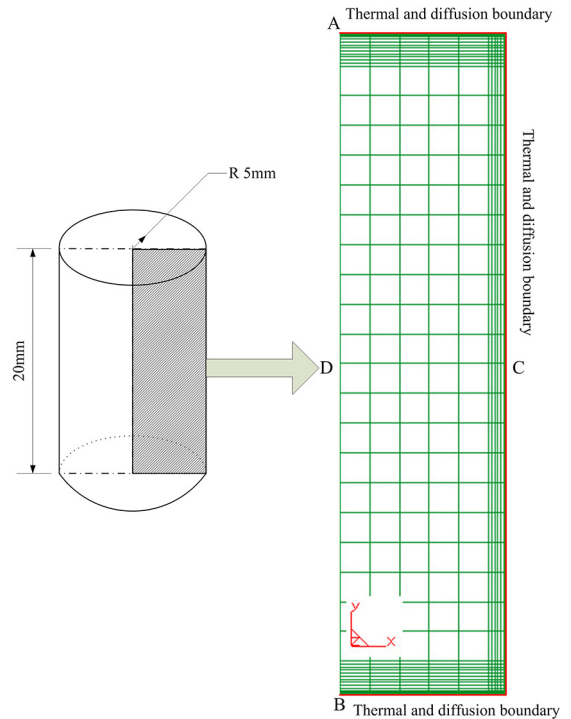


Figure 2. FEM model and meshes.

4.1. Diffusion calculations

Figure 3 depicts the evolution of the nitrogen concentration profile versus depth for gas nitriding for S30C steel. Figure 3(a) shows the contour fill by COSMAP, the nitrogen concentration gradient is hard to observe on the surface. The reason is that the considerable reduction of diffusivity when ferrite is transformed into γ' . It is observed that the nitrogen concentration gradient is steep by magnification of one rectangular. The Figure 3(b) shows the comparison between the simulated and experimental data. Although there are detailed discrepancies, it can be seen that good agreement is achieved between the numerical results and EPMA measured results.

4.2. Microstructure and hardness results

SEM observation in 300mm depth evidenced the existence of γ' (Figure 4). It can be seen that the nitride layer is composed of the thinner compound layer (ϵ -Fe_{2.3}(C, N)) and inner

Table 1. Chemical weight compositions of S30C.

Chemical elements	Fe	C	Si	Mn	Cr	P	S	Ni
Wt%	balance	0.30	0.25	0.75	0.1	0.003	0.0035	0.2

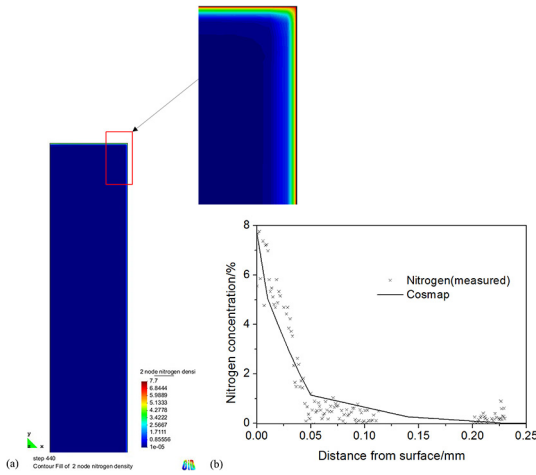


Figure 3. Simulated nitrogen concentrations by COSMAP.

diffusion layer ($\alpha + \gamma'$). The compound layer which has a thickness of about 20 μm is formed on top of the diffusion zone where dense and fine precipitates of γ' iron nitrides are present inside the ferrite grains. The corresponding simulated results are shown in Figure 5. Although the distributions of γ' in SEM are more homogeneous, the simulated depth of γ' are reasonably consistent with the SEM results. One possible explanation of inconsistent distributions is that a phenomenological equation (equation (3)) is employed in the present model. In addition, it is neglected that the replacement of some nitrogen atoms in iron-nitrogen phase by larger carbon atoms. Besides γ' phase, the compound layer

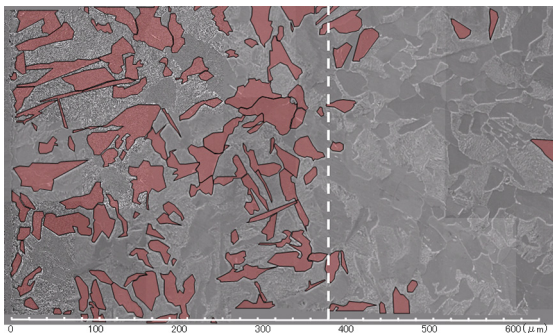


Figure 4. Cross sectional SEM observation of the nitrided specimen.

also contains a thinner ϵ phase layer. It can be seen from Figure 6 that depth of ϵ phase is around 20 μm .

Hardness profiles after nitriding are calculated by an experimental regression equation (5) and are shown in Figure 7 for S30C steel. The calculated hardness data result in good agreement with the measured ones in the compound layer and substrate. However, there are discrepancies between calculations and observations in critical diffusion layers. The measured values are greater than the calculated ones. The problem probably lies in the precipitation of fined alloy nitride (such as CrN) in the diffusion zone, which can increase hardness in diffusion layers significantly. As shown in Figure 4-7, it can be concluded that the FEM model can be employed to

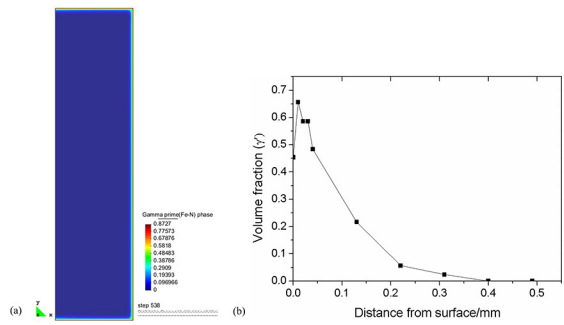


Figure 5. Simulated γ' iron nitride results by COSMAP.

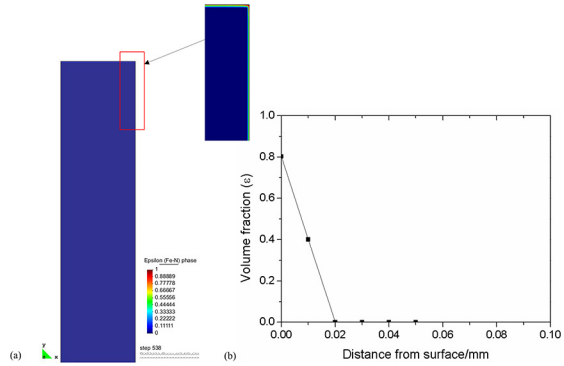


Figure 6. Simulated ϵ iron nitride results by COSMAP.

predict the nitrogen content and the nitride layer depth in the nitriding process.

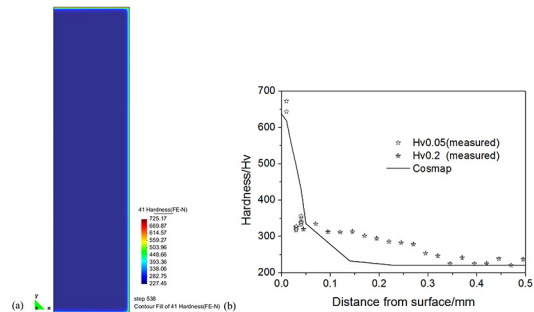


Figure 7. Simulated hardness results by COSMAP.

4.3. Interpolation results

To validate the interpolation program, the different FEM mesh size is employed to model the nitriding process of S30C steel. Processing temperature and time are the same as the previous calculations. The FEM model and mesh are shown in Figure 8. The number of elements for coarse and fine meshes is 600 and 1800 respectively. Figure 9 shows the comparisons of the simulated nitrogen concentration among the fine mesh results, the coarse mesh results and interpolated results. Compared to the results of coarse mesh, the interpolated results can illustrate better the distributions of nitrogen in the surface. It also indicates that of nitrogen concentration results of the interpolated and fine meshes are consistent.

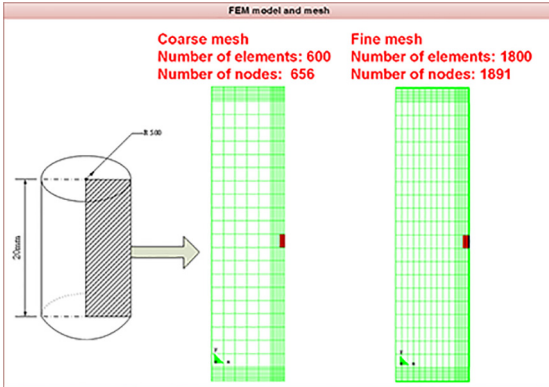


Figure 8. Schematic of coarse and fine FEM mesh.

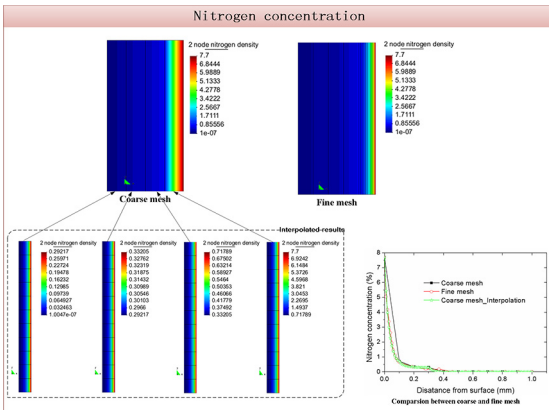


Figure 9. Comparisons of nitrogen concentrations for different meshes size.

5. Conclusions

A modified finite element model in nitriding of plain carbon steel has been developed to simulate nitrogen concentration distributions, phase formation and hardness. The model is employed to model the nitriding process of S30C steel. The simulated results are in reasonable agreement with the experimentally measured ones and theoretical analysis. Furthermore, a FEM post-process technology is developed to avoid the limit of FEM mesh improvement and time-saving by the LRA and the modified IDW method. The comparisons between fine mesh and interpolated simulated results show that the FEM post-process technology is viable. In addition, in the present model only consider the effect of carbon elements on the diffusion process of nitriding, whilst the influence of alloy elements and the precipitation of alloy nitride are not incorporated in the model. These will obviously affect the accuracy of the model and implement into the model in forthcoming studies.

6. Acknowledgements

This research receives ongoing support from the High-tech Research Center and project of nanotechnology at the Saitama

Institute of Technology, and it is sponsored by the National Natural Science Foundation of China (Project 51301121), Natural Science Foundation of Tianjin City (No. 13JCYBJC38900), Scientific Research Starting Foundation of Tianjin University of Technology and Education (No. KJY1307) and Innovation Team Training Plan of Tianjin Universities and colleges (Grant No. TD12-5043).

7. References

1. Pye D. *Practical Nitriding and Ferritic Nitrocarburizing*. Materials Park: ASM International; 2003. 256 p.
2. Somers MAJ, Mittemeijer EJ. Layer-growth kinetics on gaseous nitriding of pure iron: Evaluation of diffusion coefficients for nitrogen in iron nitrides. *Metallurgical and Materials Transactions A*. 1995;26(1):57-74.
3. Dimitrov VI, D'Haen J, Knuyt G, Ouayyaegens C, Stals LM. Modeling of nitride layer formation during plasma nitriding of iron. *Computational Materials Science*. 1999;15(1):22-34.
4. Yan M, Yan J, Bell T. Numerical simulation of nitrided layer growth and nitrogen distribution in ϵ -Fe₂N, γ -Fe₃N and α -Fe during pulse plasma nitriding of pure iron. *Modelling and Simulation in Materials Science and Engineering*. 2000;8:491.
5. Keddad M. Surface modification of the pure iron by the pulse plasma nitriding: Application of a kinetic model. *Materials Science and Engineering: A*. 2007;462(1-2):169-173.
6. Cavaliere P, Zavarise G, Perillo M. Modeling of carburizing and nitriding processes. *Computational Materials Science*. 2009;46(1):26-35.
7. Hassani-Gangaraj SM, Guagliano M. Microstructural evolution during nitriding, finite element simulation and experimental assessment. *Applied Surface Science*. 2013;271:156-163.
8. Liu CC, Ju DY, Inoue T. A Numerical Modeling of Metallothermo-mechanical Behavior in Both Carburized and Carbonitrided Quenching Processes. *ISIJ International*. 2002;42(10):1125-1134.
9. Ju DY, Liu CC, Inoue T. Numerical modeling and simulation of carburized and nitrided quenching process. *Journal of Materials Processing Technology*. 2003;143-144:880-885.
10. Deng XH, Ju DY. Prediction of Phase Composition and Nitrogen Concentration During the Nitriding Process in Low-Alloy Steel. *Materials Research*. 2016;19(2):353-359.
11. Shepard D. A two-dimensional interpolation function for irregularly-spaced data. In: *Proceedings of 23rd ACM National Conference*; 1968 Aug 27-29; Las Vegas, NV, USA. New York; 1968. p. 517-524.
12. Masjukov AV, Masjukov VV. Multiscale modification of Shepard's method for multivariate interpolation of scattered data. In: *Proceedings of 10th International Conference Mathematical Modelling and Analysis and 2nd International Conference Computational Methods in Applied Mathematics*. 2005 Jun 1-5; Trakai, Lithuania. p. 467-472.
13. Pál L, Oláh-Gál R, Makó Z. Shepard interpolation with stationary points. *Acta Universitatis Sapientiae, Informatica*. 2009;1(1)5-13.